

# An application of $L_2$ nonlinear control and gain scheduling to erbium doped fiber amplifiers

Nem Stefanovic<sup>a,\*</sup>, Min Ding<sup>b</sup>, Lacro Pavel<sup>a</sup>

<sup>a</sup>University of Toronto, Toronto, Ont., Canada M5S 3G4

<sup>b</sup>University of Toronto, Toronto, Ont., Canada M5S 2E4

Received 23 May 2006; accepted 27 January 2007

Available online 30 March 2007

## Abstract

This paper presents an application of control theory towards suppressing cross-gain modulation effects in erbium doped fiber amplifiers (EDFAs). These effects arise due to sudden input power changes at network reconfiguration or system faults. An extended nonlinear model of the EDFA is derived, including amplified spontaneous emission (ASE). Two novel EDFA control applications are developed and compared: one based on  $L_2$  nonlinear control and the other based on optimized gain scheduling. The design of each control law is subject to realistic physical constraints as encountered in industrial application.

© 2007 Elsevier Ltd. All rights reserved.

*Keywords:* Nonlinear control; PID controllers; Linearization; Optical amplifiers; Optical fiber networks; Interpolation approximation

## 1. Introduction

Regarded as the greatest innovation since optical fiber in the past decade, the erbium doped fiber amplifier (EDFA) has revolutionized the optical communication industry by enabling amplification of many lightwave channels simultaneously (Ramaswami & Sivarajan, 2002). An EDFA is an optical fiber usually a few meters in length that has been doped with erbium ions ( $\text{Er}^{3+}$ ) (Giles & Desurvire, 1991). However, there are a number of challenges that must be overcome as WDM optical networks are transformed from static point-to-point systems into dynamic, reconfigurable networks, and EDFA control is one such challenge. When information is dynamically routed through fiber links (Ramaswami & Sivarajan, 2002), data channels are expected to be added and dropped at designated points in the network with minimal power transients occurring (Srivastava, Sun, Zyskind, & Sulhoff, 1997; Sun & Srivastava et al., 1997). During channel add/drop, the EDFA suffers from cross-gain modulation which induces

power transients on surviving channels (Sun, Zyskind, & Srivastava, 1997). These unwanted power transients are detrimental to channel performance and control schemes have been realized to reduce them (Ding & Pavel, 2005; Motoshima et al., 1997, 2001; Sun & Zyskind et al., 1997). Though effective, these methods lack a systematic consideration of plant characteristics, virtually all being based on conventional proportional-integral-derivative (PID) and linearization techniques. The EDFA is a nonlinear, multivariable system, whose behavior is highly dependent on its operating point. Thus, there is a need for more systematic and sophisticated control that results in robust and dynamic EDFA devices operating over a wide range of conditions. This is the problem that is addressed in this paper. Preliminary results appeared in Stefanovic and Pavel (2005) and Ding and Pavel (2005).

Current control design approaches start with a linearized EDFA model and ignore the amplified spontaneous emission (ASE) noise. The EDFA model is developed here as a full nonlinear system with ASE. Based on this extended, nonlinear EDFA model, two control schemes are developed. The first one is a nonlinear  $L_2$  control scheme based on (Doyle, Francis, & Tannenbaum, 1993; Doyle, Glover, Khargonekar, & Francis, 1989; Khalil, 2002; Lu & Doyle,

\*Corresponding author. Tel.: +1 416 274 8265.

E-mail addresses: [nem@control.toronto.edu](mailto:nem@control.toronto.edu) (N. Stefanovic), [min.ding@utoronto.ca](mailto:min.ding@utoronto.ca) (M. Ding), [pavel@control.toronto.edu](mailto:pavel@control.toronto.edu) (L. Pavel).

1993; van der Schaft, 1991, 1992) that minimizes the variation of the average inversion level. This ensures that the channel gains remain constant. The second control scheme is used for comparison and it is an optimized gain scheduling approach. Instead of interpolating among several pre-designed controllers, a single parameterized PID controller is derived based on the known EDFA system model. The two control schemes are compared via simulations. The  $L_2$  nonlinear control shows promising results when compared to the gain scheduled PID, producing faster and smoother transient responses. This paper presents an example of a practical industrial problem tackled by using  $L_2$  nonlinear control.

This paper is organized as follows. In Section 2, an extended EDFA model is developed that includes the effect of ASE. In Section 3, the design specifications are stated and the two control schemes are developed. Simulation results from the two schemes are compared and contrasted in Section 4, followed by conclusions.

## 2. Plant specification and modeling

### 2.1. EDFA model with ASE

In this section, a state-space model for the EDFA including the ASE contribution is developed. As a starting point, the steady-state nonlinear model (Feng et al., 2002) and the basic propagation and rate equations in Giles and Desurvire (1991) are used. This new extended EDFA model will be used for control design.

The basic mechanisms in an EDFA are stimulated emission, which amplifies the signal, and spontaneous emission, which causes noise (Agrawal, 1997; Giles & Desurvire, 1991). ASE is the result of excited atoms releasing energy without stimulus from the input channel powers and it produces noise (Ramaswami & Sivarajan, 2002). ASE can have a significant effect under certain conditions of EDFA operation and manifests itself prominently with higher average inversion levels (Agrawal, 1997). A large channel drop increases the magnitude of the ASE present on the output channels.

Let  $n_i(r, \phi, z)$  for  $i = 1, 2, t$  denote the ground state, excited state and total erbium ion populations, respectively, with  $n_1 + n_2 = n_t$ . Also, let  $i_k$  denote the normalized optical intensity. Here  $r$  is the radius,  $\phi$  is the azimuth angle, and  $z$  is the distance along the EDFA fiber (Giles & Desurvire, 1991).  $P_k(z)$  will denote the power of the  $k$ th beam of light, or the channel power, as a function of distance along the EDFA fiber. Let  $\nu_k$  denote the frequency of the light beam centered at  $\lambda_k = c/\nu_k$  and  $\sigma_{ak}$  and  $\sigma_{ek}$  are the absorption and emission cross sections, respectively.

The EDFA rate and propagation equations (Giles & Desurvire, 1991) are

$$\frac{dn_2}{dt} = \sum_k \frac{P_k i_k \sigma_{ak}}{h\nu_k} n_1(r, \phi, z) - \sum_k \frac{P_k i_k \sigma_{ek}}{h\nu_k} n_2(r, \phi, z) - \frac{n_2(r, \phi, z)}{\tau_o}, \quad (1)$$

$$\frac{\partial P_k}{\partial z} = u_k \sigma_{ek} \int_0^{2\pi} \int_0^\infty i_k(r, \phi) n_2(r, \phi, z) r dr d\phi (P_k(z) + m h \nu_k \Delta \nu_k) - u_k \sigma_{ak} \int_0^{2\pi} \int_0^\infty i_k(r, \phi) \cdot n_1(r, \phi, z) r dr d\phi (P_k(z)), \quad (2)$$

where  $\tau_o$  is the spontaneous lifetime of the excited erbium atoms,  $u_k$  represents either the forward (+1) or reverse (−1) direction of propagation through the EDFA.  $m$  represents the number of modes in the fiber, and set to 2 here.  $\Delta \nu_k$  represents the effective noise bandwidth, and is set to 100 GHz here.

Eqs. (1) and (2) by themselves cannot be used for control. In Feng et al. (2002), a model was derived that includes an ASE term, but it was not placed in state-space form, nor was the ASE term used. In Appendix, a new extended EDFA model with ASE in state-space form is derived, given in its final form as

$$\dot{x} = -\frac{x}{\tau_o} - \frac{1}{\zeta \tau_o L} \sum_k \left( -g_k m \Delta \nu_k L x + u_k \left[ \frac{-g_k m \Delta \nu_k x}{(\alpha_k + g_k)x - \alpha_k} \times (1 - e^{u_k \{(\alpha_k + g_k)x - \alpha_k\} L}) + (e^{u_k \{(\alpha_k + g_k)x - \alpha_k\} L} - 1) Q_k^{in} \right] \right),$$

$$Q_k^{out} = \frac{-g_k m \Delta \nu_k x}{(\alpha_k + g_k)x - \alpha_k} [1 - e^{u_k \{(\alpha_k + g_k)x - \alpha_k\} L}] + e^{u_k \{(\alpha_k + g_k)x - \alpha_k\} L} Q_k^{in}, \quad (3)$$

where  $x = \overline{N_2}(t) = 1/L \int_0^L N_2(z, t) dz$  is the average inversion defined as the average fraction of atoms in the upper energy level, and  $Q_k^{in}$  and  $Q_k^{out}$  represent the normalized input and output powers of the  $k$ th EDFA channels, respectively.

The standard EDFA model (Sun & Zyskind et al., 1997), typically used for PID control is

$$\rho S L \left( \frac{d}{dt} + \frac{1}{\tau_o} \right) x = Q_{pump}(t) - \sum_{k=1}^N Q_k^{in}(t) \{ e^{[(g_k + \alpha_k)x - \alpha_k] L} - 1 \},$$

$$Q_k^{out}(t) = Q_k^{in}(t) e^{[(g_k + \alpha_k)x - \alpha_k] L} \quad k = 1, \dots, N, \quad (4)$$

$$G(t) = \frac{Q_{total}^{out}(t)}{Q_{total}^{in}(t)},$$

where

$$Q_{total}^{in}(t) = \sum_{k=1}^N Q_k^{in}(t), \quad Q_{total}^{out}(t) = \sum_{k=1}^N Q_k^{out}(t)$$

with  $G(t)$  being the total gain.

The new EDFA model (3) shows some interesting features when compared to the simplified model (4). There are two new terms in the state equation, and one new term in the output equation in (3). These terms are due to ASE contribution and they are independent of the input power.

### 3. Controller designs

In this section the two control schemes are outlined: the  $L_2$  nonlinear control scheme and the gain scheduled PID control scheme.

#### 3.1. $L_2$ control application

As an objective for the  $L_2$  nonlinear control scheme, consider controlling the average inversion. By keeping the average inversion constant, the output powers of each channel remain constant, as seen from (3). The control signal is the pump power, which typically should not have a response time faster than 1–10  $\mu$ s.

First, background of fundamental  $L_2$  control theory is reviewed. Next, an extended EDFA system model with a designed performance output equation is constructed. Finally, the linear  $H_\infty$  control design and the nonlinear  $L_2$  solution is then presented.

##### 3.1.1. $L_2$ nonlinear control background

$L_2$  nonlinear control (Khalil, 2002; Lu & Doyle, 1993; Pavel, 1996; Pavel & Fairman, 1996; van der Schaft, 1991, 1992) is an extension of  $H_\infty$  control to nonlinear systems. The objective is to attenuate disturbance effects on the state and performance outputs. The full information problem (FI) (Doyle et al., 1989; Lu & Doyle, 1993; Pavel & Fairman, 1996) system is defined as

$$\begin{cases} \dot{\mathbf{x}} = f(\mathbf{x}) + g_1(\mathbf{x})\mathbf{w} + g_2(\mathbf{x})\mathbf{u}, \\ \mathbf{z} = h_1(\mathbf{x}) + k_{11}(\mathbf{x})\mathbf{w} + k_{12}(\mathbf{x})\mathbf{u}, \\ \mathbf{y} = [\mathbf{x}^T \ 0]^T + [0 \ \mathbf{w}^T]^T. \end{cases} \quad (5)$$

Here,  $\mathbf{w}$ ,  $\mathbf{u}$ ,  $\mathbf{z}$ , and  $\mathbf{y}$  represent the disturbance and control input, performance, and measured output. For the FI problem, the state is directly available for measurement. System (5), has an  $L_2$  gain van der Schaft, 1992,  $\gamma$ , from  $\mathbf{w}$  to  $\mathbf{z}$ , if

$$\int_0^T \|\mathbf{z}(t)\|^2 dt \leq \gamma^2 \int_0^T \|\mathbf{w}(t)\|^2 dt, \quad (6)$$

where  $\|\cdot\|$  denotes a euclidean norm.

Theorem 3.1 of (Pavel, 1996) (or see Pavel & Fairman, 1996) provides a general  $L_2$  control solution for the FI system. This result is used in this paper and is restated below as Theorem 1.

**Theorem 1.** Assuming  $k_{12}(\mathbf{x})$  has full column rank, and  $\mathbf{S}_1(\mathbf{x}) < 0 \quad \forall \mathbf{x} \in R^n$ , where  $\mathbf{S}_1(\mathbf{x}) = \mathbf{k}_{11}(\mathbf{x})^T \mathbf{k}_{11} - \gamma^2 I$ , the  $L_2$  control objective is achievable for the FI problem with feedback  $\mathbf{u} = \mathbf{F}_{2\infty}(\mathbf{x})$  provided that:

- (1)  $\exists V(\mathbf{x}) \geq 0$ ,  $V(0) = 0$  solution of the Hamilton–Jacobi inequality (HJI)  $H_{FI}(V, \mathbf{x}) \leq 0$ , (7), with  $V_x(\mathbf{x})$  denoting  $dV(\mathbf{x})/d\mathbf{x}$ :

$$H_{FI}(V, \mathbf{x}) = V_x(\mathbf{x})f(\mathbf{x}) - \mathbf{F}_{\infty}^T(\mathbf{x})\mathbf{S}(\mathbf{x})\mathbf{F}_{\infty}(\mathbf{x}) + h_1^T(\mathbf{x})h_1(\mathbf{x}). \quad (7)$$

- (2)  $\dot{\mathbf{x}} = f(\mathbf{x}) + g(\mathbf{x})\mathbf{F}_{\infty}(\mathbf{x})$  is asymptotically stable, where

$$\begin{aligned} \mathbf{F}_{\infty}(\mathbf{x}) &= [\mathbf{F}_{1\infty}^T(\mathbf{x}) \ \mathbf{F}_{2\infty}^T(\mathbf{x})]^T = -\mathbf{S}^{-1}(\mathbf{x}) \\ &\times \left[ \frac{1}{2} g^T(\mathbf{x}) V_x^T(\mathbf{x}) + k_1^T(\mathbf{x}) h_1(\mathbf{x}) \right], \end{aligned}$$

$$\mathbf{S}(\mathbf{x}) = k_1^T(\mathbf{x})k_1(\mathbf{x}) - \begin{bmatrix} -\gamma^2 I & 0 \\ 0 & 0 \end{bmatrix},$$

$$k_1(\mathbf{x}) = [k_{11}(\mathbf{x}) \ k_{12}(\mathbf{x})],$$

$$g(\mathbf{x}) = [g_1(\mathbf{x}) \ g_2(\mathbf{x})].$$

##### 3.1.2. FI problem construction for EDFA

In the following, the EDFA model (3) is associated to the FI problem (5). A standard nonlinear shift will be used later in the paper to denote  $x = 0$ ,  $\mathbf{w} = 0$  and  $u = 0$  as the equilibrium point to generate a specific average inversion level,  $x_0$ , with particular input powers. The value of the state  $x$  can be directly computed in real-time using measurements of the input and output powers on a particular channel.

Next, choose a performance output,  $\mathbf{z}$ , such that  $k_{12}(x)$  has full column rank and  $\mathbf{S}_1(x) < 0$ . An appropriate choice is to attenuate both  $x$  and  $u$ . Hence set

$$\mathbf{z} = [x^T \ 0]^T + \beta [0 \ u^T]^T \quad (8)$$

such that the  $L_2$  gain (6) from the disturbance inputs,  $\mathbf{w}$ , to the state,  $x$ , and pump power,  $u$ , is attenuated. Here,  $\beta$  is an arbitrary scalar, and it is set to unity.  $H_{FI}(V, x)$  (7) is stated as

$$H_{FI}(V, x) = A_{FI}(x) \frac{dV(x)}{dx} + \frac{1}{4} \frac{dV(x)}{dx} Q_{FI}(x) \frac{dV(x)}{dx} + R_{FI}(x), \quad (9)$$

where,  $A_{FI}(x) = f(x)$ ,  $Q_{FI}(x) = (1/\gamma^2)g_1(x)g_1^T(x) - g_2(x)g_2^T(x)$ ,  $R_{FI}(x) = x^2$  and  $f(x)$ ,  $g_1(x)$ ,  $g_2(x)$  are appropriately defined from the right-hand side of (3) after the nonlinear shift from  $x_0$  (see Table 1).

##### 3.1.3. Linear FI problem solution

It is shown in van der Schaft (1991) that the linearized  $\gamma$  is valid on some neighborhood of the nonlinear system. Thus, linearizing and solving for  $\gamma$  directly, the results will be extended to the nonlinear system. In the following, the linear terms of a nonlinear  $f(x)$  will be denoted by using a capital letter, i.e.  $\mathbf{F}$ . Taking only the linear terms of the HJE,  $H_{FI}(V, x) = 0$ , (9), the linear Riccati equation is obtained:

$$\mathbf{A}^T \mathbf{P} + \mathbf{P} \mathbf{A} + \mathbf{P} \mathbf{Q}_{FI} \mathbf{P} + \mathbf{R} = 0. \quad (10)$$

From basic  $H_\infty$  theory (Doyle et al., 1993), restrict  $\mathbf{Q}_{FI} \leq 0$  and solve for  $\mathbf{P} > 0$ . From this restriction on  $\mathbf{Q}_{FI}$ , an explicit restriction for  $\gamma$  can be written as

$$\gamma \geq \sqrt{\frac{\mathbf{G}_1 \mathbf{G}_1^T}{\mathbf{G}_2 \mathbf{G}_2^T}} \quad (11)$$

Table 1  
Nonlinear EDFA system terms

| Terms      | Expression  |
|------------|---|
| $f(x)$ :   | $-\frac{x}{\tau_o} - \frac{1}{\zeta\tau_oL} \sum_k \left( -g_k m \Delta v_k L x + u_k \left[ \frac{-g_k m \Delta v_k x}{(\alpha_k + g_k)x - (\alpha_k + \ell_k)} (1 - e^{u_k((\alpha_k + g_k)x - (\alpha_k + \ell_k))L}) \right] \right)$ |
| $g_1(x)$ : | $-\frac{1}{\zeta\tau_oL} [u_1 (e^{u_1((\alpha_1 + g_1)x - (\alpha_1 + \ell_1))L} - 1) \dots u_N (e^{u_N((\alpha_N + g_N)x - (\alpha_N + \ell_N))L} - 1)]$   |
| $g_2(x)$ : | $-\frac{1}{\zeta\tau_oL} u_{\text{pump}} (e^{u_{\text{pump}}((\alpha_{\text{pump}} + g_{\text{pump}})x - (\alpha_{\text{pump}} + \ell_{\text{pump}}))L} - 1)$   |

Note that here,  $\mathbf{G}_1$  and  $\mathbf{G}_2$  represent the linear parts of  $g_1(x)$  and  $g_2(x)$  and hence are not functions of  $x$ , but are constants. The above relation would not be very useful if a static, unsatisfactory lower bound for  $\gamma$  is given. To address this, arbitrary scaling is introduced on the pump input and disturbances. Let the scaled channel power and pump power disturbances be  $\Delta \mathbf{w} = X_w \mathbf{w}$  and  $\Delta u = X_u u$ , where  $X_w$  and  $X_u$  are scaling factors. The EDFA model in FI form (5) is rewritten as

$$\begin{cases} \dot{x} = f(x) + \frac{g_1(x)}{X_w} (\Delta \mathbf{w}) + \frac{g_2(x)}{X_u} (\Delta u), \\ \mathbf{z} = [x^T \ 0]^T + [0 \ 1]^T (\Delta u), \\ \mathbf{y} = [x^T \ 0]^T + [0 \ I]^T (\Delta \mathbf{w}). \end{cases}$$

The scaling terms  $X_w$  and  $X_u$  are considered as positive scalar values for simplicity. Based on this scaling, the  $\gamma$  variable can be manipulated. Notice that  $A_{FI}(x)$  and  $R_{FI}(x)$  are not affected by the scaling factors. With scaling, (11) becomes

$$\gamma \geq \frac{X_u}{X_w} \sqrt{\frac{\mathbf{G}_1 \mathbf{G}_1^T}{\mathbf{G}_2 \mathbf{G}_2^T}}. \quad (12)$$

The  $\gamma$  that achieves equality in (12) represents  $\gamma_{\min}$ , the smallest possible  $\gamma$  for a valid solution. The following expression must be satisfied (van der Schaft, 1991):

$$\|x\|^2 + \|\Delta u\|^2 \leq \gamma^2 \|\Delta \mathbf{w}\|^2, \quad (13)$$

where  $\|\cdot\|$  denotes a Euclidean norm. Now, substituting  $\gamma_{\min}$  from (12) into (13) and using the scaling notation, we obtain

$$\|x\| \leq \left( \frac{X_u}{X_w} \sqrt{\frac{\mathbf{G}_1 \mathbf{G}_1^T}{\mathbf{G}_2 \mathbf{G}_2^T}} + \varepsilon \right) \|\Delta \mathbf{w}\|, \quad (14)$$

where  $\varepsilon$  is a non-negative value. The controller,  $u = -\mathbf{G}_2^T \mathbf{P} x$ , from (van der Schaft, 1991) solves the linearized FI problem, and this is a linearization of the full nonlinear controller in Theorem 1.

### 3.1.4. Nonlinear FI solution

If the linearized  $H_{FI}$  is solved, there exists a neighborhood about the operating point such that (13) is satisfied for a nonlinear controller (van der Schaft, 1991). A positive value,  $0.2x^2$ , is added to  $R_{FI}(x)$  to solve the HJI (9) as a specific HJE. This is done by extending results in Lukes

(1969) and Pavel (1996) based on Taylor approximation. In Lukes (1969), it was proven inductively that the solution of each Taylor term coefficient for  $V(x)$  is calculable given the previous coefficients of  $V(x)$ .

Two conditions must be satisfied according to Theorem 1. If the solution of the HJI,  $H_{FI}(V, x) \leq 0$ , (9), is found, then the second condition is that

$$\dot{x} = f(x) + \frac{1}{2} \mathbf{Q}_{FI}(x) V_x(x) \quad (15)$$

is asymptotically stable. The first term in (15),  $f(x)$ , defined in (9), has a stable vector field over the state space (Khalil, 2002). If it can be guaranteed that the second term in (15) has a stable vector field, or an unstable vector field that does not have sufficient magnitude to overcome the first term, then the second condition of Theorem 1 is satisfied. This can be done by examining the geometry of the terms over the state space.

$\mathbf{Q}_{FI}(x)$  (9) is manipulated by increasing the  $\gamma$  value from its minimum value, but its multiplicative influence on  $V_x(x)$  (see Theorem 1 conditions) is unclear because  $V(x)$  is not known in advance. However, a few inferences can be made. First of all, since the linear part is valid,  $V(x)$  will satisfy  $V(x_0) = 0$  and  $V(x) > 0$  at least in some region around  $x_0$ . The shape is parabolic in this region, so that  $V_x(x) = 0$  and  $V_x(x) < 0$  for  $x < 0$ , and  $V_x(x) > 0$  for  $x > 0$  in a neighborhood of  $x_0$ . If a  $V(x)$  can be obtained that looks parabolic, all that would be necessary is to make  $\mathbf{Q}_{FI} < 0 \ \forall x$  (assuming  $\frac{1}{2} \mathbf{Q}_{FI}(x) V_x(x)$  is stable, or of sufficiently small magnitude). From the structure of  $\mathbf{Q}_{FI}$  (9), notice that the first term is positive, and the second term is negative. Hence, if the second term dominates the first, then the objective is achieved. The final nonlinear solution is obtained by tuning and iteration.

### 3.2. Gain scheduling control

In this section a gain scheduling PID scheme optimized for the EDFA at any operating condition is presented. This will be used for comparison with  $L_2$  nonlinear controller. The design objective is to keep the output power of each channel constant and to limit the settling time to less than 1 ms when up to 97% of the input power is dropped or added. The real-time information available to this controller is the total input and total output powers since these are typical measurements used in the industry at amplifier sites (Pavel, 2003). By maintaining a constant total gain,

(4), the gain and the output power of each channel remains approximately constant.

### 3.2.1. Plant linearization

Based on (4), a linearized model is generated for a nominal operating condition ( $x^o$ ,  $Q_{pump}^o$ ,  $G^o$ ,  $Q_k^{ino}$ , and  $Q_k^{outo}$ ,  $\forall k = 1, 2, \dots, N$ ). The pump power and the total gain after linearization are treated as control input ( $u$ ) and output ( $y$ ):

$$\begin{aligned} \frac{dx(t)}{dt} &= A\Delta x(t) + \mathbf{B}_1 \mathbf{Q}^{in}(t) + \mathbf{B}_2 u(t), \\ \mathbf{Q}^{out}(t) &= \mathbf{C}_1 \Delta x(t) + \mathbf{D}_{11} \mathbf{Q}^{in}(t) + \mathbf{D}_{12} u(t), \\ y(t) &= \mathbf{C}_2 \Delta x(t) + \mathbf{D}_{21} \mathbf{Q}^{in}(t) + \mathbf{D}_{22} u(t), \end{aligned} \quad (16)$$

where  $\Delta x(t) = x(t) - x^o$ ,  $\mathbf{Q}^{in}(t) = Q^{in}(t) - Q^{ino}$ ,  $u(t) = Q_{pump}(t) - Q_{pump}^o$ ,  $\mathbf{Q}^{out}(t) = Q^{out}(t) - Q^{outo}$ ,  $y(t) = G(t) - G^o$  and all parameters are given in Table 2.

The transfer function from  $u$  to  $y$  can be rewritten as  $G(s) = K_p / (s + \omega_{OL})$  with

$$\begin{aligned} K_p &= \frac{\sum_{k=1}^N Q_k^{outo} (g_k + \alpha_k) L}{SL\rho Q_{total}^{ino}}, \\ \omega_{OL} &= \frac{1}{\tau_o} \left\{ 1 + \frac{\tau_o}{S\rho} \sum_{k=1}^N Q_k^{outo} (g_k + \alpha_k) \right\} \end{aligned} \quad (17)$$

depending on the operating point.

A PID controller in cascade form is designed

$$PID : K_{PID}(s) = K_r \frac{(1 + \tau_1 s)(1 + \tau_2 s)}{\tau_1 s(1 + 0.1\tau_2 s)}. \quad (18)$$

In order to increase the phase margin of the loop-gain function,  $G(s)K_{PID}(s)$ , from simulations it is found that  $\tau_1 = 1/5\omega_{OL}$  and  $\tau_2 = 3/50\omega_{OL}$  are optimal. This ensures a minimum phase margin of  $50^\circ$ . With a simple single-pole plant, direct calculation by pole placement (Skogestad & Postlethwaite, 1996) is used. The characteristic equation of the closed-loop system is given as

$$\tau_1 s(1 + 0.1\tau_2 s)(s + \omega_{OL}) + K_p K_r (1 + \tau_1 s)(1 + \tau_2 s) = 0. \quad (19)$$

Since the dynamics change for different operating conditions  $K_r$  is normalized first with respect to  $\omega_{OL}$ . Therefore, take  $K_p K_r$  chosen to be proportional to  $\omega_{OL}$ ,  $K_p K_r = C\omega_{OL}$  with  $C$  a constant to be designed. Using these into (19), for desired closed-loop poles and the root locus

method, the optimal  $C$  is found, which places the closed-loop poles at  $7.6\omega_{OL}$ ,  $7.6\omega_{OL}$ , and  $491\omega_{OL}$ . The parameters of the PID controller are summarized in Table 3.

### 3.2.2. Gain scheduling

The EDFA model is a highly nonlinear system. For typical parameter ranges,  $\omega_{OL}$  (17) varies from 1000 rad/s to 10 000 rad/s. A controller designed for a single operating point is not sufficient to effectively control the EDFA over the entire range of operating conditions. Typically, a classical gain scheduling approach (Rugh, 1991) is based on linearizing the nonlinear system at several operating points and designing a linear controller for each point, and then interpolating, or “scheduling”, the linear controllers. In the EDFA case, interpolation is bypassed because controller parameters have been derived for any operating point (Table 3). The plant  $G(s)$  has its gain and pole (17) as functions of  $Q_k^{ino}$ ,  $Q_k^{outo}$ , and  $x^o$ . An estimate of  $K_p$  and  $\omega_{OL}$  (17) is obtained from the parameters directly measured, i.e.  $Q_{total}^{in}(t)$ ,  $Q_{total}^{out}(t)$  and  $G(t)$ , by first rewriting

$$K_p = \frac{\overline{g + \alpha} \rho G^o}{S}, \quad \omega_{OL} = \frac{1}{\tau_o} \left\{ 1 + \frac{\tau_o}{S\rho} \overline{g + \alpha} Q_{total}^{ino} G^o \right\}, \quad (20)$$

where  $G^o = Q_{total}^{outo} / Q_{total}^{ino}$  and  $\overline{g + \alpha} = \sum_{k=1}^N (Q_k^{outo} / Q_{total}^{outo}) (g_k + \alpha_k)$ . From values of  $g_k$  and  $\alpha_k$ ,  $\overline{g + \alpha}$ , attains a value from 1.28 to 2.91. This value is approximated by the mean of its attainable range, i.e. 2.09. From (20), the plant can be represented by two measurable parameters,  $Q_{total}^{in}(t)$  and  $G(t)$ , which are used as the scheduling variables.

## 4. Simulations and discussions

In this section, the open-loop response of the nonlinear system with ASE (3) is analyzed then the  $L_2$  nonlinear controller and the gain scheduled PID controller are compared. The following parameters are used in all simulations: channels = 32, channel powers  $P_{in,k} = 42.6 \mu\text{W}$ ,

Table 3  
The PID controller’s parameters

| Parameters | $K_r$                         | $\tau_1$                 | $\tau_2$                  |
|------------|-------------------------------|--------------------------|---------------------------|
| PID        | $\frac{33.8\omega_{OL}}{K_p}$ | $\frac{1}{5\omega_{OL}}$ | $\frac{3}{50\omega_{OL}}$ |

Table 2  
Expressions for the parameters of the linear model of the EDFA

$$\begin{aligned} A &= \frac{-1}{\tau_o} \left\{ 1 + \frac{\tau_o}{S\rho} \sum_{k=1}^N Q_i^{ino} e^{((g_k + \alpha_k)x^o - z_k)L} (g_k + \alpha_k) \right\}, \quad B_1(k, 1) = \frac{Q_k^{ino} - Q_k^{outo}}{Q_k^{ino} SL\rho}, \quad B_2 = \frac{1}{SL\rho} \\ C_1(1, k) &= Q_k^{outo} (g_k + \alpha_k) L, \quad D_{11}(i, j) = \begin{cases} \frac{Q_i^{outo}}{Q_i^{ino}}, & i = j, \\ 0, & \text{else} \end{cases} \quad D_{12} = 0 \\ C_2 &= \frac{\sum_{k=1}^N Q_k^{outo} (g_k + \alpha_k) L}{Q_{total}^{ino}}, \quad D_{21}(1, k) = \frac{e^{((g_k + \alpha_k)x^o - z_k)L}}{Q_{total}^{ino}} - \frac{Q_{total}^{outo}}{(Q_{total}^{ino})^2}, \quad D_{22} = 0 \end{aligned}$$

$P_{pump} = 150$  mW, fiber length  $L = 13$  m. The data for the EDFA are listed in Table 4.

#### 4.1. Open-loop response of EDFA model with ASE

The four major terms of the state equation (3) without state dynamics are plotted on a logarithmic scale in Fig. 1. The linear terms are represented by the two parallel looking plots. The term with the singularity in the middle is the input power term. The singularity is the result of the value 0 on a logarithmic scale. This term is the most dominant. The most interesting plot is given by the nonlinear ASE term (dotted). It starts as the smallest term, then grows to be the second largest. Since the input term is dependent on the input powers, the nonlinear ASE term

Table 4  
EDFA Parameters, signal and pump bands

| (a) EDFA parameters                   |                     |                    |
|---------------------------------------|---------------------|--------------------|
| Core radius                           | 1.8                 | $\mu\text{m}$      |
| Er radius                             | 1.7                 | $\mu\text{m}$      |
| Er ion density, $\rho$                | $4.33\text{E} + 24$ | ions/ $\text{m}^3$ |
| Metastable lifetime, $\tau$           | 10                  | ms                 |
| Channel separation (for $\Delta\nu$ ) | 0.75                | nm                 |
| (b) EDFA signal and pump bands        |                     |                    |
| Pump band                             | absorption          | emission           |
| Wavelength (nm)                       | alpha (dB/m)        | $g^*$ (dB/m)       |
| 980                                   | 3.229               | 0                  |
| Signal band                           | absorption          | emission           |
| Wavelength (nm)                       | alpha (dB/m)        | $g^*$ (dB/m)       |
| 1530.072                              | 6.49342764          | 6.3508087          |
| $\vdots$                              | $\vdots$            | $\vdots$           |
| 1565.072                              | 1.64433299          | 3.29519786         |

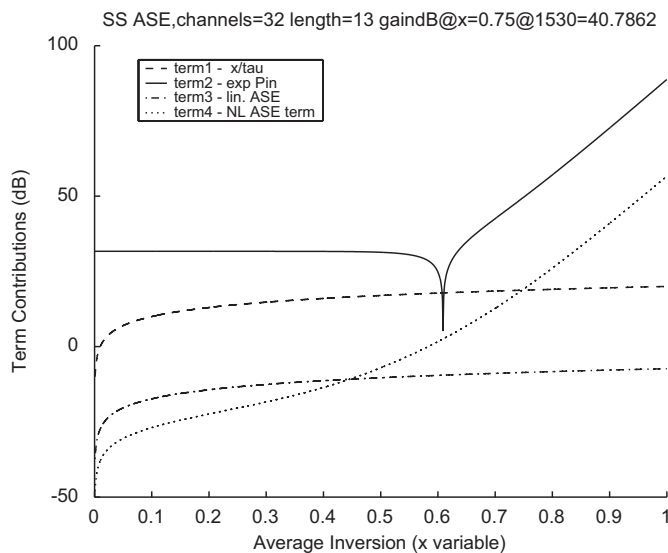


Fig. 1. ASE model state equation terms in steady state.

may have a significant effect on the state equation for relatively low input powers at high inversion levels. This confirms ASE experiments (Desurvire & Simpson, 1989).

Open-loop responses for two main channel drop situations; 50% and 97% channel drops are shown in Fig. 2. Fig. 2(c) shows also the full failure case where 100%, or 32 channels, are dropped. Channel add cases are similar to drop cases.

Note the different impacts that ASE has in Fig. 2. For a 50% drop, the effect of ASE is small. The ASE component grows larger for the 97% drop case and is the largest for the 100% drop case. The magnitude of the ASE in the 100% drop case surpasses that of channel output powers for the 50% drop case. If the variation in the state  $x$  is controlled, then the variation in ASE is restricted. The 100% channel drop case is a special example that represents total channel failure at the EDFA input. It corresponds to the extreme increase in the ASE magnitude seen in Fig. 1. Since EDFAs are interconnected in optical networks, such a channel failure could result in a disturbance to other EDFAs in the network. If uncontrolled, the transient could propagate down an EDFA chain and increase its transient speed through the fiber length as demonstrated in Srivastava et al. (1997) and Sun and Srivastava et al. (1997).

#### 4.2. $L_2$ controller design with parameters constrained to physical limitations

The design constraint for the EDFA  $L_2$  nonlinear controller, is the pump's ability to deliver power over a specified time scale. By simulation, a nonlinear  $L_2$  gain of 0.03 yields 15  $\mu\text{s}$  pump response time. By design, choose scaling terms  $X_w$  and  $X_u$  that give an  $L_2$  gain of 0.003 for the linearized system, and then increase the  $L_2$  gain to 0.03 to satisfy the nonlinear conditions. From the EDFA model, (3), and the data in Table 4, the operating point,  $x_0 = 0.60725$ , is calculated and a standard nonlinear shift is performed to set  $x_0 = 0$ . Also  $\Delta w = 0$  and  $\Delta u = 0$  represent the signal powers and pump powers that define the operating point.

The linear  $H_\infty$  control is used as a first step in the design process. Denote  $G_1$  and  $G_2$  as the linear part of  $g_1(x)$  and  $g_2(x)$ , and use (14) to obtain  $X_u$ . Choose the  $L_2$  gain,  $\gamma = 0.003$  to get  $X_u = 4.1169 \times 10^{-21}$ . If the value of  $\gamma$  is increased, then  $Q_{FI}(x)$  can be made more negative to achieve an  $L_2$  gain over a larger neighborhood. So  $\gamma$  is increased until the requirements for Theorem 1 are obtained, which gives  $\gamma = 0.03$ . A global solution is not needed, since simulations show that the controller functions properly in the worst case channel drop. The final controller used is

$$u_{32} = -1.0237x + 7.8867(10^{-1})x^2 + 3.1106x^3 - 9.95(10^1)x^4 - 6.8735(10^2)x^5 + 2.6259(10^2)x^6 + 7.586(10^2)x^7. \quad (21)$$

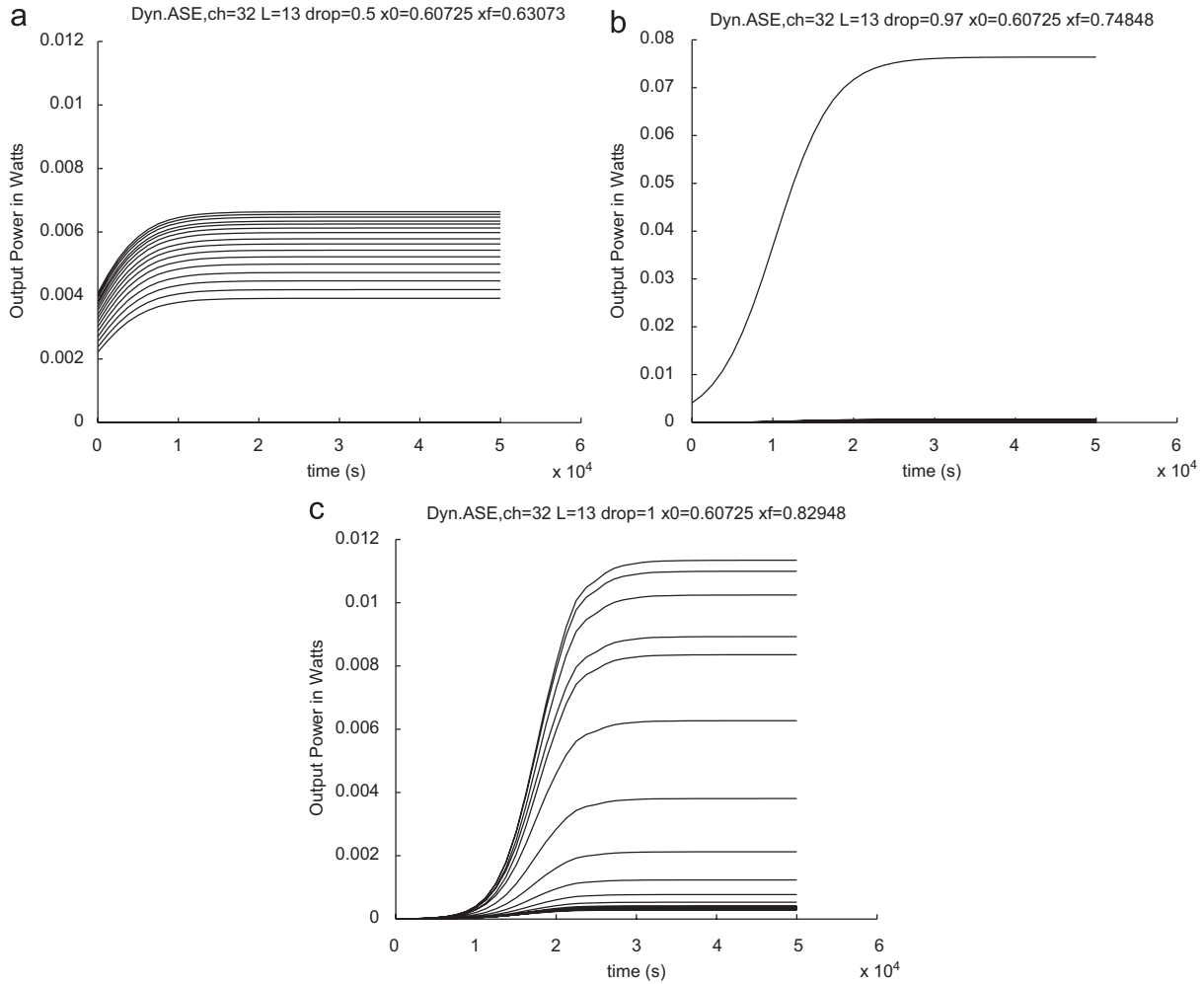


Fig. 2. Open-loop output power responses for channel drops with ASE. (a) Dynamic ASE model response with 50% channel drop. (b) Dynamic ASE model response with 97% channel drop. (c) Dynamic ASE model response with 100% channel failure.

### 4.3. Simulation results comparison

The results for 50% and 97% channel drop are shown in Figs. 3 and 4. Both PID scheduled controller and nonlinear  $L_2$  controller results are shown in the same figure. In both cases, the  $L_2$  nonlinear controller clearly outperforms the linear gain scheduled PID controller achieving shorter transient time (15  $\mu$ s compared to up to 30  $\mu$ s in Fig. 3 and 1.2 ms in Fig. 4 for the scheduled PID controller) and much smoother response. This advantage is maintained when compared to other existent EDFA control schemes. In Motoshima et al. (2001), a 0.8 dB change in output power given a channel drop from 32 to 3 channels occurs assuming a controller response time of 20  $\mu$ s. The  $L_2$  nonlinear controller ensures 0.3 dB suppression for a 15  $\mu$ s response time. In Tran, Chae, Tucker, and Wen (2005), the output power transients are suppressed to within 1.0 dB in  $\leq 5 \mu$ s. The  $L_2$  nonlinear control law can be made to operate within  $\leq 5 \mu$ s with an even smaller output power suppression within 0.3 dB. Hence, the  $L_2$  nonlinear control law is competitive with the most recent EDFA control

schemes, and even surpasses them in performance. On the contrary, the gain scheduled PID controller generates spikes in the total gain and the pump power at the instance of channels dropping. This is because the PID controller acts upon the change of the total gain, which varies instantaneously when channels drop. Notice the pump power stays at zero for a short period in the PID controlled cases to reduce the average inversion as fast as possible. Fig. 3 shows a power change of approximately  $-0.6$  dB for the PID gain scheduling which is not as efficient as the  $L_2$  nonlinear controller, but falls below the 0.8 dB reference (Motoshima et al., 2001).

Two more observations can be made from the simulation results. First, note that the  $L_2$  nonlinear controller yields similar responses in both cases whereas the scheduled PID controller shows a great variation as seen in Fig. 4. The reason is that the open-loop pole with only one input channel is much smaller than for the previous plant with 32 input channels which causes longer transient time for PID control. Secondly, the final values of the pump and channel output power are different in the two control schemes. This is reasonable

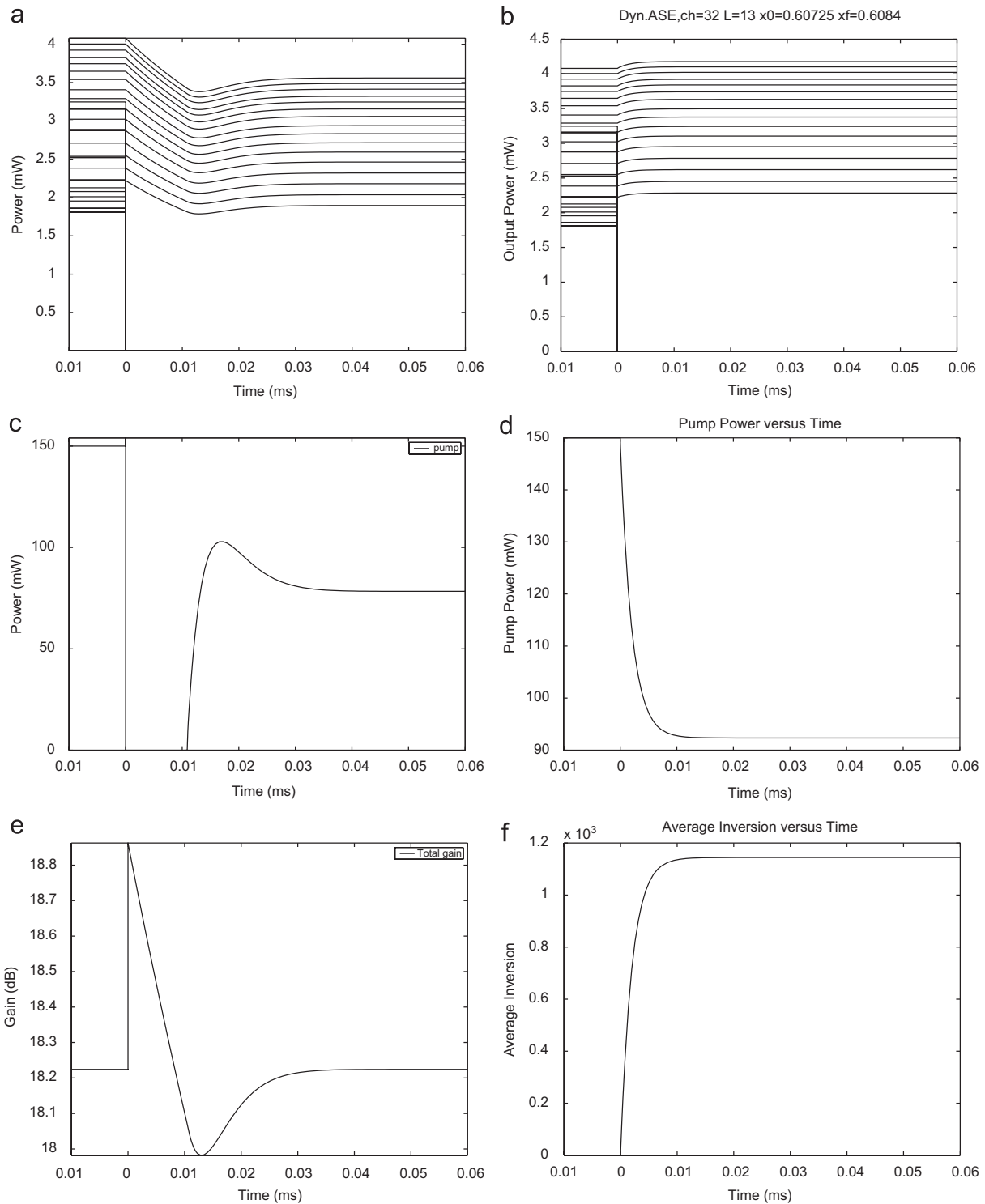


Fig. 3. System response with 16 channel dropped from 32 channels: (a)  $p^{out}$ , 32 channels, PID controller; (b)  $p^{out}$  of 32 channels with controller; (c)  $p_{pump}$  with PID controller; (d)  $p_{pump}$  with  $L_2$  controller; (e) total gain, G, with PID controller; (f) average inversion with  $L_2$  controller.

because the objective of the scheduled PID controller is to clamp the total gain, whereas the  $L_2$  nonlinear controller tries to minimize the change of the average inversion.

As a remark, it can be noted that the channel add behavior is very similar to the channel drop behavior and does not contribute to any new insight. In the additional case, there is a decrease in the average inversion level, so

the pump compensates by increasing its power, as opposed to decreasing it for the channel drop case.

### 5. Conclusion

In this paper, transient control in erbium doped fiber amplifiers (EDFAs) was considered. A new EDFA model

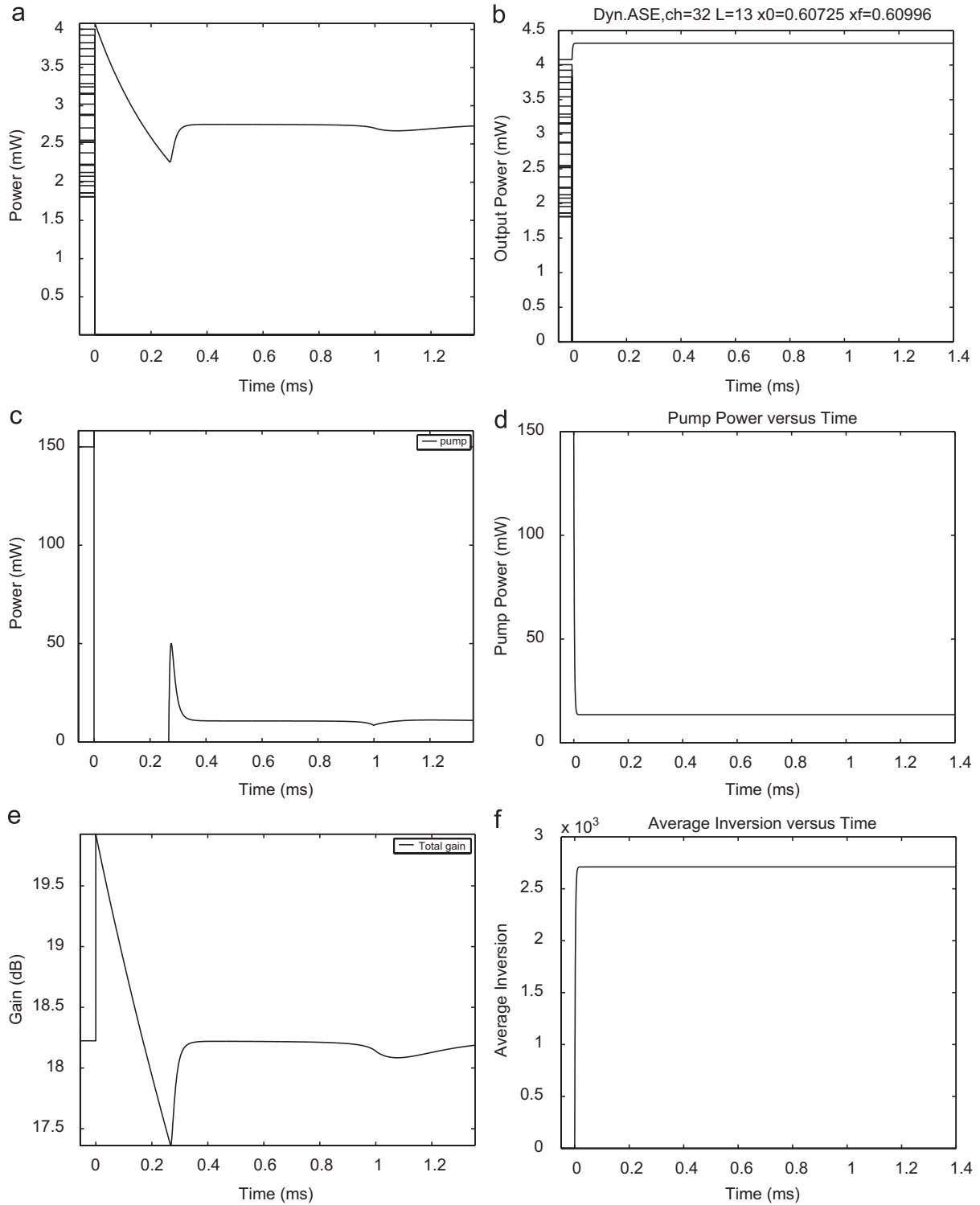


Fig. 4. System response with 31 channels dropped from 32 channels: (a)  $p^{out}$ , 32 channels, PID controller; (b)  $p^{out}$  of 32 channels with  $L_2$  controller; (c)  $p_{pump}$  with PID controller; (d)  $p_{pump}$  with  $L_2$  controller; (e) total gain,  $G$ , with PID controller; (f) average inversion with  $L_2$  controller.

that incorporates ASE was derived. Situations such as high average inversion level coupled with a large channel drop have been shown to generate significant ASE contribution. As such, it has been shown that it is necessary to include ASE in the EDFA system model to more accurately describe EDFA operation.

Based on this model an  $L_2$  nonlinear control scheme has been analyzed and compared to a gain scheduling PID control scheme. The  $L_2$  nonlinear control method restricts changes in the EDFA state variable. The design of both control laws was subject to realistic physical constraints and limitations. Simulation results were presented that

compared the controller performances and highlighted their trade-offs. The  $L_2$  controller consistently outperforms the gain scheduled controller in transient response as well as smoothness of control power. This is justified by the fact that the ASE model is more complete, and the  $L_2$  controller takes into account the nonlinear nature of the EDFA system.

### Acknowledgments

This work is supported by the Natural Science and Engineering Research Council of Canada.

### Appendix A. Derivation of EDFA system model with amplified spontaneous emission

The following assumptions are made: The erbium population is uniformly distributed in a disk of radius  $b$  (Giles & Desurvire, 1991) and along the length of the fiber (Sun & Zyskind et al., 1997). Thus,  $n_i$  represents the average erbium concentration along the radius, angle and length of the fiber.

Let the absorption and gain spectra be,  $\alpha_k$  and  $g_k$ , (Giles & Desurvire, 1991).

$$\alpha_k = \sigma_{ak} \int_0^{2\pi} \int_0^\infty i_k(r, \phi) n_i(r, \phi, z) r dr d\phi, \quad (\text{A.1})$$

$$g_k = \sigma_{ek} \int_0^{2\pi} \int_0^\infty i_k(r, \phi) n_i(r, \phi, z) r dr d\phi. \quad (\text{A.2})$$

Then from (1), (2) and (A.1), (A.2) the following PDE equations are obtained with respect to  $z$  and  $t$ :

$$\left( \frac{\partial}{\partial t} + \frac{1}{\tau_o} - \frac{1}{\zeta \tau_o} \sum_k g_k m \Delta v_k \right) \frac{n_2}{n_t} = \frac{-1}{\zeta \tau_o} \sum_k u_k \frac{1}{h\nu_k} \frac{\partial P_k}{\partial z}, \quad (\text{A.3})$$

$$\frac{\partial P_k}{\partial z} = u_k P_k(z) \left\{ (\alpha_k + g_k) \frac{n_2}{n_t} - \alpha_k \right\} + u_k g_k \frac{n_2}{n_t} m h \nu_k \Delta v_k, \quad (\text{A.4})$$

where  $n_2$  denotes the average inversion level,  $\zeta = \rho S / \tau$  is the saturation parameter,  $\rho$  is the density of active erbium atoms and  $S$  is the fiber cross-sectional area.

First, solve for  $P_k$  explicitly from (A.4). Define

$$Q = -u_k \left\{ (\alpha_k + g_k) \frac{n_2}{n_t} - \alpha_k \right\}, \quad R = u_k g_k \frac{n_2}{n_t} m h \nu_k \Delta v_k. \quad (\text{A.5})$$

So that (A.4) becomes

$$\frac{\partial P_k(z)}{\partial z} = -Q P_k(z) + R \quad (\text{A.6})$$

Then, power at the end of the fiber,  $P_k(L)$  can be obtained from (A.6) as

$$P_k(L) = e^{-H(L)} \left\{ \int_0^L e^{H(z)} R(z) dz + P_k(0) \right\}, \quad (\text{A.7})$$

where  $H(z) = \int_0^z Q(p) dp$  and  $H(L) = Q(z)L$ , or using (A.5) expressed as

$$P_k(L) = \frac{-g_k(n_2/n_t) m \nu_k \Delta v_k}{(\alpha_k + g_k)(n_2/n_t) - \alpha_k} [1 - e^{u_k \{ (\alpha_k + g_k)(n_2/n_t) - \alpha_k \} L}] + e^{u_k \{ (\alpha_k + g_k)(n_2/n_t) - \alpha_k \} L} P_k(0). \quad (\text{A.8})$$

Now the rate equation (A.3) is a PDE with respect to  $z$  and  $t$ . Integrating both sides with respect to  $z$  along the length of the fiber and normalizing by  $L$  gives

$$\left( \frac{\partial}{\partial t} + \frac{1}{\tau_o} - \frac{1}{\zeta \tau_o} \sum_k g_k m \Delta v_k \right) x = \frac{-1}{\zeta \tau_o L} \sum_k u_k \frac{1}{h\nu_k} (P_k(L) - P_k(0)),$$

where  $x = (1/L) \int_0^L (n_2/n_t) dz$  is the average inversion level taken as the state variable.  $Q_k = P_k/h\nu_k$  is the normalized power or photon flux (Giles & Desurvire, 1991). Using (A.8), the state-space EDFA model with ASE is obtained as in (3), with  $Q_k^{\text{in}} = P_k(0)/h\nu_k$ ,  $Q_k^{\text{out}} = P_k(L)/h\nu_k$  the normalized input and output powers of the  $k$ th EDFA channels.

Note that by forcing  $\Delta v_k = 0$  (noise bandwidth) in (3), this extended model becomes the simplified model without ASE from (Sun & Zyskind et al., 1997), given in (4). The control input is separated as a channel at a separate wavelength with pump power  $P_{\text{pump}}(t)$ ,  $Q_{\text{pump}}(t) = P_{\text{pump}}(t)/h\nu_{\text{pump}}$ .

### References

- Agrawal, G. P. (1997). *Fiber-optic communication systems*. New York: Wiley.
- Desurvire, E., & Simpson, J. R. (1989). Amplification of spontaneous emission in erbium-doped single-mode fibres. *Journal of Lightwave Technology*, 7(5), 835–845.
- Ding, M., & Pavel, L. (2005). Gain scheduling control design of an erbium-doped fibre amplifier by pump compensation. In *Proceedings of the IEEE conference on control applications* (pp. 510–516).
- Doyle, J. C., Francis, B. A., & Tannenbaum, A. R. (1993). *Feedback Control Theory*. New York: Maxwell Macmillan.
- Doyle, J. C., Glover, K., Khargonekar, P. P., & Francis, B. A. (1989). State-space solutions to standard  $H_2$  and  $H_\infty$  control problems. *IEEE Transactions on Automatic Control*, 34(8), 831–847.
- Feng, X., Jin, T., Wang, Y., Wang, Q., Liu, X., Peng, J., 2002. A simple control algorithm for wide-band channel-power clamped EDFA. *Optics Communications*, (213), 285–292.
- Giles, C. R., & Desurvire, E. (1991). Modeling erbium-doped fiber amplifiers. *Journal of Lightwave Technology*, 9(2), 271–283.
- Khalil, H. K. (2002). *Nonlinear systems*. New Jersey: Prentice-Hall.
- Lu, W. M., & Doyle, J. C. (1993).  $H_\infty$  control of nonlinear systems via output feedback: A class of controllers. In *Proceedings of the 32nd conference on decision and control* (pp. 166–171).
- Lukes, D. L. (1969). Optimal regulation of nonlinear dynamical systems. *SIAM Journal on Control*, 7(1), 75–100.
- Motoshima, K., Shimizu, K., Takano, K., Mizuochi, T., Kitayama, T., & Ito, K. (1997). Automatic gain control of erbium-doped fiber amplifiers for wdm transmission systems. *IEICE Transactions on Communications*, E80B(9), 1311–1319.
- Motoshima, K., Suzuki, N., Shimizu, K., Kasahara, K., Kitayama, T., & Yasui, T. (2001). A channel-number insensitive erbium-doped fiber

- amplifier with automatic gain and power regulation function. *Journal of Lightwave Technology*, 19(11), 1759–1767.
- Pavel, L. (1996). Nonlinear  $H_\infty(L_2)$  control with applications. Ph.D. dissertation, Queens University, Kingston, Ontario.
- Pavel, L. (2003). Control design for transient power and spectral control in optical communication networks. In *Proceedings of the IEEE conference on control applications*, Vol. 1 (pp. 415–422).
- Pavel, L., & Fairman, F. W. (1996). Robust stabilization of nonlinear plants—an  $L_2$  approach. *International Journal of Robust and Nonlinear Control*, 6, 691–726.
- Ramaswami, R., & Sivarajan, K. N. (2002). *Optical networks: a practical perspective* (2nd ed). San Diego: Academic Press.
- Rugh, W. J. (1991). Analytical framework for gain scheduling. *IEEE Control Systems Magazine*, 11, 79–84.
- Skogestad, S., & Postlethwaite, I. (1996). *Multivariable feedback control: analysis and design*. Toronto: Wiley.
- Srivastava, A. K., Sun, Y., Zyskind, J. L., & Sulhoff, J. W. (1997). EDFA transient response to channel loss in WDM transmission system. *IEEE Photonics Technology Letters*, 9(3), 386–388.
- Stefanovic, N., & Pavel, L. (2005).  $L_2$  nonlinear control of edfa system with amplified spontaneous emission. In *Proceedings of the IEEE conference on control applications* (pp. 289–296).
- Sun, Y., Srivastava, A. K., Zyskind, J. L., Sulhoff, J. W., Wolf, C., & Tkach, R. W. (1997). Fast power transients in WDM optical networks with cascaded EDFAs. *Electronics Letters*, 33(4), 313–314.
- Sun, Y., Zyskind, J. L., & Srivastava, A. K. (1997). Average inversion level, modeling, and physics of erbium-doped fiber amplifiers. *IEEE Journal of Selected Topics Quantum Electronics*, 3, 991–1007.
- Tran, A. V., Chae, C.-J., Tucker, R. S., & Wen, Y. J. (2005). Average inversion level, modeling, and physics of erbium-doped fiber amplifiers. *IEEE Photonics Technology Letters*, 17(1), 226–228.
- van de Schaft, A.J., 1991. On a state space approach to nonlinear  $H_\infty$  control. *Systems and Control Letters*, (16), 1–8.
- van der Schaft, A. J. (1992).  $L_2$ -gain analysis of nonlinear systems and nonlinear state feedback  $H_\infty$  control. *IEEE Transactions on Automatic Control*, 37(6), 770–784.